14th European Signal Processing Conference (EUSIPCO 2006), Florence, Italy, September 4-8, 2006, copyright by EURASIP

ON ALIASING EFFECTS IN THE CONTOURLET FILTER BANK

Truong T. Nguyen and Soontorn Oraintara

Department of Electrical Engineering, University of Texas at Arlington,
416 Yates Street, Rm 517-518, Arlington, TX 76019–0016, USA
email: nttruong@msp.uta.edu, oraintar@uta.edu, web: www-ee.uta.edu/msp

ABSTRACT

The pyramidal directional filter bank (PDFB) for the contourlet transform is analyzed in this paper. First, the PDFB is viewed as an overcomplete filter bank, and the directional filters are expressed in terms of polyphase components of the pyramidal filter bank and the conventional DFB. The aliasing effect of the conventional DFB and the Laplacian pyramid to the equivalent directional filters is then considered, and the conditions to reduce this effect are presented. Experiments show that the designed PDFBs satisfying these requirements have the equivalent filters with much better frequency responses. The performance of the new PDFB is verified by non-linear approximation of images. It is found that improvement of 0.2 to 0.5 dB in PSNR as compared to the existing PDFB can be achieved.

1. INTRODUCTION

In the past two decades, wavelets and filter banks (FB) have gained considerable interest in signal processing, partly due to the ability of wavelet functions and their associated regular FBs to optimally represent one-dimensional piecewise smooth signals. However, the separable wavelets are not effective in capturing line discontinuities since they cannot take advantage of the geometrical regularity of image structures. Image transitions such as edges and textures are expensive to represent through wavelets. Therefore, integrating the geometric regularity in the image representation is a key challenge to improve the performances of current image coders.

Recently, Candès and Donoho constructed the curvelet transform [1], and proved that it is an essentially optimal representation of two-variable functions, which are smooth except at discontinuities along $\boldsymbol{C}^2$ (twice differentiable) curve. The nonlinear approximation of a function f, $f_M^{(c)}$, reconstructed by M curvelet coefficients has an asymptotic decay rate of $\|f - f_M^{(c)}\|^2 \leq CM^{-2}(\log_2 M)^3$. This decay rate of the approximation error is a significant theoretical improvement compared to those by wavelet or Fourier coefficients, which are $O(M^{-1})$ and $O(M^{-1/2})$, respectively [2]. Since the space of smooth functions with singularities along $\boldsymbol{C}^2$ curves is similar to natural images with regions of continuous intensity value and discontinuous along smooth curves (edges), there is strong motivation for finding similar transform in the discrete domain [3].

In [4], Do and Vetterli proposed the pyramidal directional filter bank (PDFB) to implement the contourlet transform. The proposed structure of the PDFB is a combination of the Laplacian pyramid [5] and the conventional DFB [6]. It unites the advantages of both structures, which are multiresolution and multidirection. The authors also show that the contourlet transform can achieve the asymptotic optimal result as the curvelet transform. Essentially, these conditions assume that the directional filters have good bandpass and stopband characteristics in the Fourier domain.

Since the main motivation for the new image basis are its effectiveness in representing natural image, there are already several attempts to employ the PDFB in image coding [7, 8, 9]. These works are based on the original implementation of the PDFB [4], which contains some aliasing in the directional filters. Therefore, the achieved coding results are not comparable to state-of-the-art wavelet based coders, such as JPEG2000.

Paper outline. In Section 2, the PDFB is viewed as an overcomplete FB, and the equivalent directional filters are expressed in terms of the polyphase components of the filters used in the PDFB structure. The aliasing problems existing in the PDFB structure are analyzed in Section 3, where it is shown that most of the aliasing can be removed if the two lowpass filters employed in the pyramid satisfy the Nyquist criteria. Discussion and simulations in Section 4 demonstrate the improvement of the PDFB with new design conditions. The paper is concluded in Section 5.

A note on notation. Bold face lower case letters are used to represent vectors, and bold face upper case letters are reserved for matrices. For example $H(\boldsymbol{\omega})$ is equivalent to $H(\omega_1, \omega_2)$. The superscripts ^{T} and $^{-T}$ denote the transpose and transpose of the inverse operators, respectively. $\mathcal{N}(\boldsymbol{Q})$ is the set of integer vectors in the region $\boldsymbol{Qt}$ where $\boldsymbol{t} \in [0, 1)^2$. $|\boldsymbol{Q}|$ represents the determinant of the matrix $\boldsymbol{Q}$. The matrix exponential $\boldsymbol{z}^{\boldsymbol{M}}$ is defined as

$$\boldsymbol{z}^{\boldsymbol{M}} \triangleq [z_1^{m_{11}} z_2^{m_{21}}, z_1^{m_{12}} z_2^{m_{22}}]^T, \tag{1}$$

where $\boldsymbol{M} = \begin{bmatrix} m_{11} & m_{12} \\ m_{21} & m_{22} \end{bmatrix}$. On the unit circle $\boldsymbol{z}^{\boldsymbol{M}}$ is equivalent to $\boldsymbol{M}^T\boldsymbol{\omega} = [m_{11}\omega_1 + m_{21}\omega_2, m_{12}\omega_1 + m_{22}\omega_2]^T$. $\boldsymbol{D}_2$ is defined as $diag\{2, 2\}$ matrix. For other notations and a review of multidimensional multirate operations, the reader is referred to [10].

2. THE PYRAMIDAL DFB AS AN OVERCOMPLETE FILTER BANK

The pyramidal DFB (contourlet transform) is created by combining the Laplacian pyramid and the DFB with 2^n orientational subbands [4]. It is shown in this section that the combination of a Laplacian pyramid and a four-band DFB is equivalent to an overcomplete five-band FB. Let us write the two-dimensional lowpass filter $G(\boldsymbol{z})$ in polyphase form:

$$\begin{aligned} G(\boldsymbol{z}) &= G^{(0)}(\boldsymbol{z}^{\boldsymbol{D}_2}) + z_1^{-1}G^{(1)}(\boldsymbol{z}^{\boldsymbol{D}_2}) + z_2^{-1}G^{(2)}(\boldsymbol{z}^{\boldsymbol{D}_2}) + \\ &\quad + z_1^{-1}z_2^{-1}G^{(3)}(\boldsymbol{z}^{\boldsymbol{D}_2}) = \boldsymbol{g}^T(\boldsymbol{z}^{\boldsymbol{D}_2})\boldsymbol{e}(\boldsymbol{z}), \end{aligned}$$

This work was supported in part by NSF Grant ECS-0528964.

where $\boldsymbol{g}(\boldsymbol{z}) = [G^{(0)}(\boldsymbol{z}), G^{(1)}(\boldsymbol{z}), G^{(2)}(\boldsymbol{z}), G^{(3)}(\boldsymbol{z})]^T$ and $\boldsymbol{e}(\boldsymbol{z}) = [1, z_1^{-1}, z_2^{-1}, z_1^{-1}z_2^{-1}]^T$. Similarly, $\mathbf{f}(\mathbf{z})$ represents the column matrix of the polyphase components of the interpolation filter $F(\boldsymbol{z})$, i.e.

$$F(\boldsymbol{z}) = F^{(0)}(\boldsymbol{z}^{\boldsymbol{D}_2}) + z_1 F^{(1)}(\boldsymbol{z}^{\boldsymbol{D}_2}) + z_2 F^{(2)}(\boldsymbol{z}^{\boldsymbol{D}_2}) + \\ + z_1 z_2 F^{(3)}(\boldsymbol{z}^{\boldsymbol{D}_2}) = \boldsymbol{f}^T(\boldsymbol{z}^{\boldsymbol{D}_2})\boldsymbol{e}(\boldsymbol{z}^{-\mathbf{1}}).$$

Let us denote the detailed output of the Laplacian pyramid as $d(\boldsymbol{n})$ (see Fig. 1(a)) and $\boldsymbol{I}$ is the 4×4 identity matrix. If one considers $d(\boldsymbol{n})$ as the output of a FB with input $x(\boldsymbol{n})$ then it can be shown that the corresponding polyphase matrix is $\boldsymbol{I} - \boldsymbol{f}(\boldsymbol{z})\boldsymbol{g}^T(\boldsymbol{z})$.

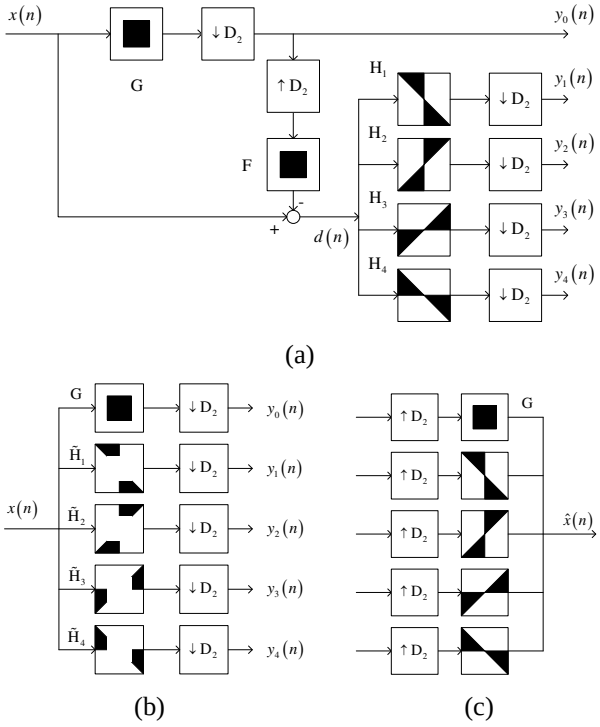

Figure 1: The four-band PDFB (a) The analysis side of the PDFB, (b) Equivalent overcomplete FB and (c) The synthesis FB.

In the PDFB depicted in Fig. 1(a), a four-band DFB is applied to the detailed signal $d(\mathbf{n})$. Let $\boldsymbol{E}(\boldsymbol{z})$ be the polyphase matrix of the four orientational filters, i.e.

$$[H_1(\boldsymbol{z}), H_2(\boldsymbol{z}), H_3(\boldsymbol{z}), H_4(\boldsymbol{z})]^T = \boldsymbol{E}(\boldsymbol{z}^{\boldsymbol{D}_2})\boldsymbol{e}(\boldsymbol{z}). \quad (2)$$

The input $x(\mathbf{n})$ goes through a Laplacian pyramid and a four-band DFB to produce four subsampled outputs $y_i(\mathbf{n})$, $i = 1, 2, 3$ and 4. These four signals can be considered as the outputs of the analysis side of a FB with input $x(\boldsymbol{n})$, and it can be shown that the polyphase matrix of this overall FB is $\tilde{\boldsymbol{E}}(\boldsymbol{z}) = \boldsymbol{E}(\boldsymbol{z})\left(\boldsymbol{I} - \boldsymbol{f}(\boldsymbol{z})\boldsymbol{g}^T(\boldsymbol{z})\right)$.

Therefore, the PDFB in Fig. 1(a) is equivalent to the structure in Fig. 1(b) with the same lowpass filter $G(\mathbf{z})$ and four directional filter $\tilde{H}_i(\mathbf{z})$ which are given as

$$[\tilde{H}_1(\boldsymbol{z}), \tilde{H}_2(\boldsymbol{z}), \tilde{H}_3(\boldsymbol{z}), \tilde{H}_4(\boldsymbol{z})]^T = \tilde{\boldsymbol{E}}(\boldsymbol{z}^{\boldsymbol{D}_2})\boldsymbol{e}(\boldsymbol{z}). \quad (3)$$

Fig. 1(c) shows the corresponding synthesis four-band DFB.

3. ALIASING ON THE PDFB

In order for the PDFB to achieve its potential performance, it is necessary that the equivalent directional filters have excellent frequency responses. In general, the implementation of the PDFB consists of a separable Laplacian pyramid and a binary-tree conventional DFB [6]. Thus, there are two sources of aliasing that will be considered in this section: those on the DFB tree, and those caused by the pyramid structure.

3.1 Aliasing on the binary tree of the conventional DFB

The conventional DFB is often realized by a binary-tree of maximally-decimated two-channel FBs [6]. Although this method has a very efficient structure, it also implies some inherent aliasing problems. It is possible to implement the tree structure with only one prototype fan FB [11]. Let us assume that one prototype fan filter is $H_0^F(\boldsymbol{\omega})$, then it can be shown that one equivalent directional filter of an eight-band DFB is

$$\tilde{H}_0(\omega_1, \omega_2) = H_0^F(\omega_1, \omega_2) H_0^F(\omega_1 + \omega_2, \omega_1 - \omega_2) \\ H_0^F(2(\omega_1 + \omega_2), 2\omega_1), \quad (4)$$

where the frequency supports of $H_0^F(\omega_1, \omega_2)$, $H_0^F(\omega_1 + \omega_2, \omega_1 - \omega_2)$, $H_0^F(2(\omega_1 + \omega_2), 2\omega_1)$ are plotted in Fig. 2(a). Assume that these filters have reasonably good frequency responses, i.e. flat in the passbands and stopbands (black and white areas), and have transition regions in between (gray areas). The resulting filter $\tilde{H}_0(\omega_1, \omega_2)$ will have a frequency support as in Fig. 2(b), which has transition bands at $\omega_2 \approx \pm\pi$.

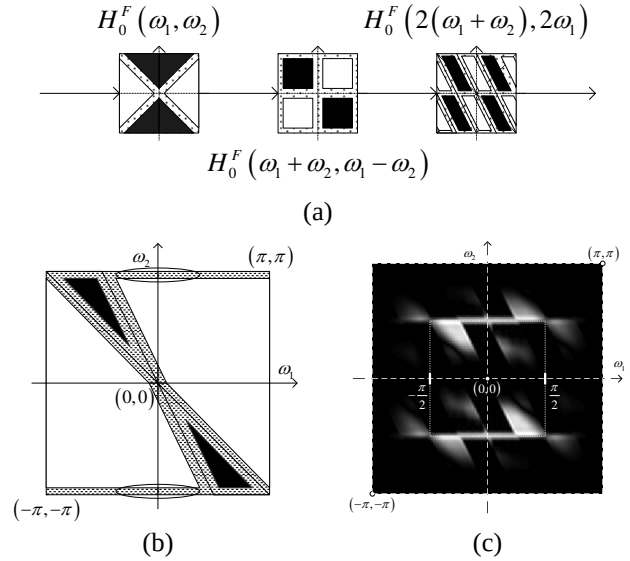

Figure 2: Aliasing effect on DFBs obtained by using the tree structure: (a) the equivalent product filter of one subband (obtained by using the noble identity), (b) the equivalent directional filter $\tilde{H}_0(\omega_1, \omega_2)$. Black, gray and white colors denote passband, transition band and stopband, respectively, and (c) an example of equivalent PDFB filter at the second resolution level.

This aliasing problem is more obvious in the directional filters of the second resolution of the PDFB if the lowpass

filter $G(\boldsymbol{\omega})$ does not satisfy the Nyquist criteria with respect to decimation matrix $\boldsymbol{D}_2$, i.e. if its passband and transition band are not restricted within $[-\pi/2, \pi/2]^2$. The equivalent directional filters of the PDFB in [4] at the second level of the pyramid is plotted in Fig. 2(c) where the aliasing at high frequency is displayed very clearly. However, if the filter $G(\boldsymbol{\omega})$ is designed to satisfy the Nyquist sampling criteria, the lowpass images beginning from the second level of the Laplacian pyramid will have negligible aliasing. As a result, the aliasing effect on the directional filters can be reduced.

3.2 Aliasing effect of the Laplacian pyramid

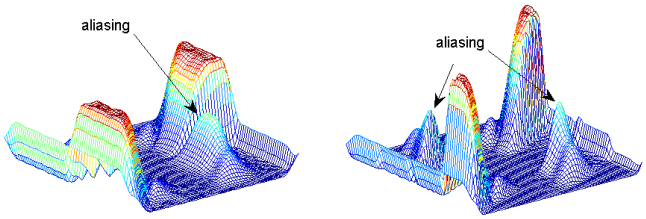

(a) (b)

Figure 3: Examples of equivalent directional filters in the PDFB (a) The equivalent filter $\tilde{H}_1(\omega_1, \omega_2)$ of four-band PDFB (b) A directional filter of eight-band PDFB. function associated with filter $\tilde{H}_1$.

In (3), the equivalent directional filters $\tilde{H}_i(\boldsymbol{z})$ can be expressed in terms of the lowpass filters $G(\boldsymbol{z})$, $F(\boldsymbol{z})$ and the four highpass filters $H_i(\boldsymbol{z})$. Let us consider a realization of the PDFB implemented using the '9-7' biorthogonal filters as the lowpass filters $G(\boldsymbol{z})$ and $F(\boldsymbol{z})$ as in [4]. The fan FBs in the DFB tree structure are implemented using the ladder structure (with filter lengths of 21 and 41) in [12]. The first directional filter for the cases of four-band DFB is plotted in Fig. 3(a). It is observed that the directional filters have 'bumps' in the stopband region. Similarly, an eight-band DFB can be obtained by cascading one more step of two-channal filter banks at the binary-tree of the DFB. Its first directional filter is presented in Fig. 3(b) showing more bumps in the stopband. It will be shown later that this effect is due to aliasing resulting from decimation and interpolation of the Laplacian pyramid, and the heights of these peaks are independent from the directional filters in the DFB.

Let $FH_1(\boldsymbol{z}) = F(\boldsymbol{z})H_1(\boldsymbol{z})$ be written in a polyphase form as

$$\begin{aligned} FH_1(\boldsymbol{z}) &= FH_1^{(0)}(\boldsymbol{z}^{\boldsymbol{D}_2}) + z_1^{-1}FH_1^{(1)}(\boldsymbol{z}^{\boldsymbol{D}_2}) \\ &\quad + z_2^{-1}FH_1^{(2)}(\boldsymbol{z}^{\boldsymbol{D}_2}) + z_1^{-1}z_2^{-1}FH_1^{(3)}(\boldsymbol{z}^{\boldsymbol{D}_2}). \end{aligned}$$

By some manipulation, it can be shown that the block diagrams in Figs. 5(a) and (b) are equivalent where $FH_1^{(0)}(\boldsymbol{z})$ is the first polyphase component of $FH_1(\boldsymbol{z})$. Consider the signal $y_1(\boldsymbol{n})$ in Fig 1(a). The corresponding block diagram can be redrawn as in Fig 4(a) where the subsystem in the dotted rectangle is equivalent to $FH_1^{(0)}(\boldsymbol{z})$. Using the noble identity, the top path in Fig 4(a) can be further simplified as in as in Fig. 4(b).

Since the PDFB is implemented with FIR filters, all the filters' frequency responses have transition bands between

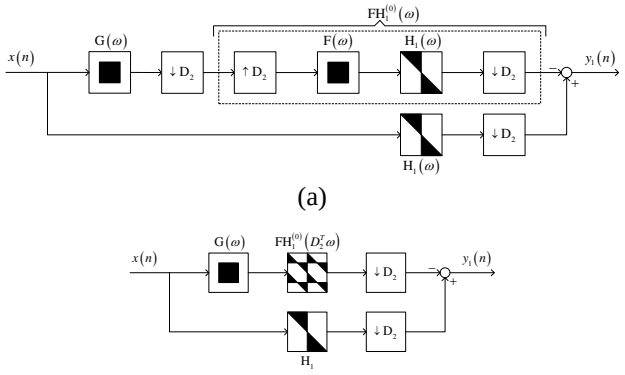

Figure 4: The equivalent structure to the directional filter $\tilde{H}_1(\omega_1, \omega_2)$ in the four-band PDFB in Fig. 1.

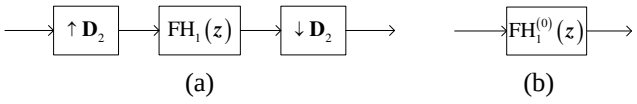

Figure 5: Equivalent block diagrams.

the stopbands and passbands. Fig. 6(a) shows the passband support of $FH_1(\mathbf{z})$ where black, gray and white correspond to passband, transition band and stopband, respectively. The resulting filter $FH_1^{(0)}(\boldsymbol{z}^{\boldsymbol{D_2}})$ in Fig 4(b) is obtained by downsampling followed by upsampling the filter $FH_1(\boldsymbol{z})$ by $\boldsymbol{D}_2$. The corresponding frequency response $FH_1^{(0)}(\boldsymbol{D}_2^T\boldsymbol{\omega})$ whose supports are displayed in Fig 6(b) can be given by

$$FH_1^{(0)}(\boldsymbol{D}_2^T\boldsymbol{\omega}) = \frac{1}{|\boldsymbol{D}_2|}\sum_{\mathbf{k}\in\mathcal{N}(\boldsymbol{D}_2^T)} FH_1(\boldsymbol{\omega} - 2\pi\boldsymbol{D}_2^{-T}\mathbf{k}). \tag{5}$$

Therefore,

$$\begin{aligned} &\tilde{H}_1(\boldsymbol{\omega}) = H_1(\boldsymbol{\omega}) - \\ &\frac{1}{|\boldsymbol{D}_2|}G(\boldsymbol{\omega})\sum_{\mathbf{k}\in\mathcal{N}(\boldsymbol{D}_2^T)} F(\boldsymbol{\omega} - 2\pi\boldsymbol{D}_2^{-T}\mathbf{k})H_1(\boldsymbol{\omega} - 2\pi\boldsymbol{D}_2^{-T}\mathbf{k}). \end{aligned} \tag{6}$$

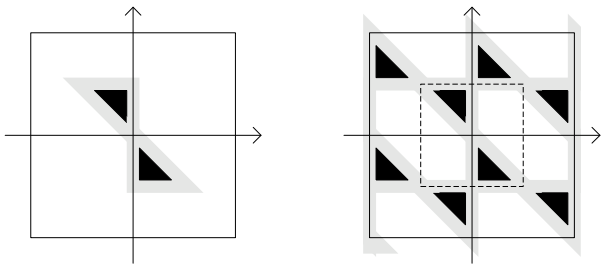

(a) (b)

Figure 6: The frequency support of (a) $FH_1(\boldsymbol{\omega})$, and (b) $FH_1^{(0)}(\boldsymbol{D}_2^T\boldsymbol{\omega})$.

Assuming that the lowpass filter $G(\boldsymbol{\omega})$ is approximately zero in its stopband regions, two of the aliasing terms in the

$$\tilde{H}_1(\omega_1,\omega_2) \approx H_1(\omega_1,\omega_2)\left(1-\frac{1}{|\boldsymbol{D}_2|}G(\omega_1,\omega_2)F(\omega_1,\omega_2)\right)-\frac{1}{|\boldsymbol{D}_2|}G(\omega_1,\omega_2)F(\omega_1,\omega_2-\pi)H_1(\omega_1,\omega_2-\pi). \quad (7)$$

summation can be neglected, and the overall filter $\tilde{H}_1(\boldsymbol{\omega})$ can be approximated by (7). The second term in (7) produces the peaks in stopband regions of $\tilde{H}_1(\boldsymbol{\omega})$ (see Fig. 3). The positions of these peaks are in the passband of the modulated directional filter $H_1(\omega_1,\omega_2-\pi)$, so the only way to eliminate these 'bumps' is to reduce the overlapping transition bands between $G(\omega_1,\omega_2)$ and $F(\omega_1,\omega_2-\pi)$. Since both $G(\boldsymbol{z})$ and $F(\boldsymbol{z})$ are lowpass, and if the Nyquist sampling condition is satisfied, the above aliasing term will be cancelled. Therefore, the two filters in the Laplacian pyramid should satisfy the following conditions:

$$G(\omega_1,\omega_2)\approx 0, \qquad \text{and} \qquad F(\omega_1,\omega_2)\approx 0 \quad (8)$$

when $|\omega_1|>\pi/2$ or $|\omega_2|>\pi/2$. This means that the cutoff frequency of $G(\boldsymbol{z})$ and $F(\boldsymbol{z})$ must be a little less than $\pi/2$ in order to keep approximately zero response beyond $\pi/2$. Let us call the conventional PDFB (with cutoff frequency at $\pi/2$) *aliasing* PDFB, and the one satisfying the above constraints *non-aliasing* PDFB.

4. EXPERIMENTS AND DISCUSSIONS

In order to demonstrate the aliasing effect from the directional filters in the PDFB, the impulse responses of the overall directional filters at different scales are plotted in Fig. 7. In the aliasing case (Fig. 7(a)), the Laplacian filters are obtained from the lowpass filters in the '9-7' biorthogonal FB, whereas in the non-aliasing case (Fig. 7(b)), the two lowpass filters $G(\boldsymbol{z})$ and $F(\boldsymbol{z})$ are defined in the frequency domain to have frequency responses approximately zero when $\omega_i>\pi/2$ and the transition band from $\pi/4$ to $\pi/2$. The DFB in both aliasing and non-aliasing PDFBs are realized by a binary tree of two-channel fan FBs, which are implemented by a two-steps ladder structure [12]. Both of the two decompositions have 32, 16, 8 and 4 directional subbands at the first, second, third and fourth resolutions, respectively. Examples of the equivalent directional filters at the four resolutions of the two PDFBs are illustrated in Fig. 7. It is evident that the filters in Fig. 7(b) have much less aliasing and better directionalities than those in Fig. 7(a).

In practice, most of the unwanted aliasing components considered in the previous section can be reduced if the two lowpass filters in the pyramid have slightly smaller passband. Figs. 8(a) and (b) show examples of the first directional filters of the four-band and eight-band PDFBs whose $F(\boldsymbol{z})$ and $G(\boldsymbol{z})$ are designed to have a transition band $0.3\pi<|\omega_i|<0.6\pi$. Comparing to the frequency responses obtained in Figs. 3(a) and (b), it is clear that those aliasing bumps have been significantly suppressed.

The aliasing effect is also demonstrated in an experiment. The coefficients obtained from the aliasing and non-aliasing PDFBs are used to approximate the *Barbara* and *Lena* images by thresholding a certain amount of smallest coefficients. The PSNRs of the reconstruction images obtained by keeping different numbers of coefficients are summarized in Table 1. It is evident that an improvement of 0.2 to 0.5 dB is achieved from using the non-aliasing PDFB.

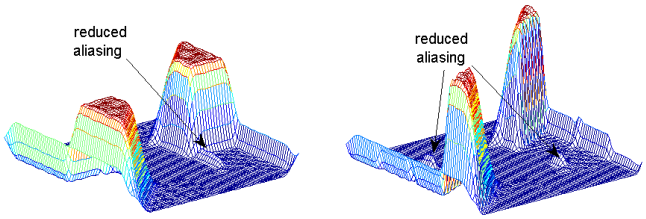

(a) (b)

Figure 8: Examples of directional filters in the PDFB (a) $\tilde{H}_1(\omega_1,\omega_2)$ of a four-band PDFB and (b) a directional filter of an eight-band PDFB.

Table 1: The nonlinear approximation of the aliasing and non-aliasing PDFBs in *Barbara* and *Lena* images in term of PSNR.

	Barbara		*Lena*	
#coeffs	Aliasing	Non-aliasing	Aliasing	Non-aliasing
1024	21.64	21.71	24.69	24.93
2048	23.18	23.41	27.19	27.27
4096	25.07	25.47	29.65	29.79
8192	27.30	27.92	32.19	32.39
16384	29.80	30.69	34.73	34.92

Although the equivalent directional filters of the PDFB (or contourlet basis) are efficient in representing image contours, it performance tends to be lower than that of the traditional discrete wavelet transform (DWT) when the image sizes get smaller. In our non-linear approximation experiment with typical testing images (Lena and Barbara), the best results are achieved when the PDFB is used at the highest resolution, and the DWT is used when the image sizes are less than or equal to 256×256. An image coder based on reduced-aliasing PDFB and DWT decomposition is reported in [13]. Experimental results show that the proposed coding algorithm outperforms the current state-of-the-art wavelet based coders, such as JPEG2000, for images with directional features.

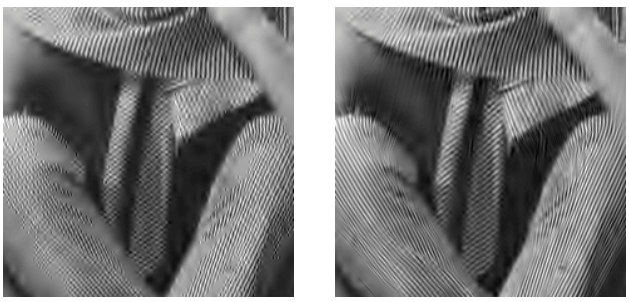

(a) (b)

Figure 9: Reconstructed Barbara images at 0.15 bpp using (a) JPEG2000, PSNR = 25.93 dB and (b) PDFB, PSNR = 26.74 dB [13].

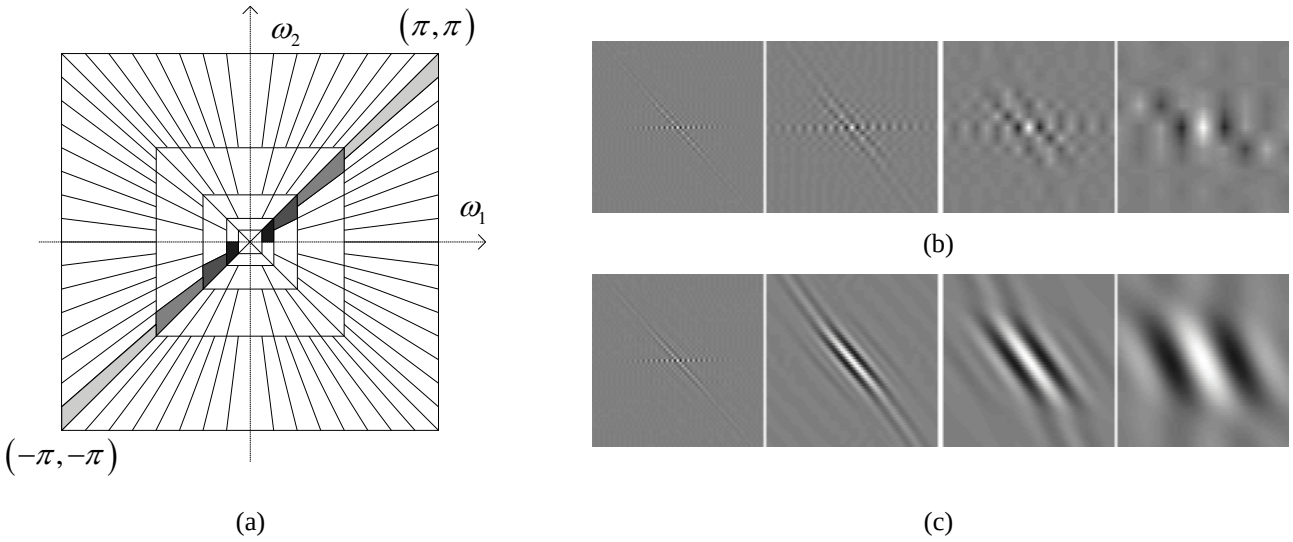

Figure 7: (a) The essential frequency supports of directional filters in the PDFB at different scales: level 1 - 32 bands, level 2 - 16 bands, level 3 - 8 bands, level 4 - 4 bands. The corresponding impulse responses in case of (b) aliasing Laplacian pyramid filters and (c) non-aliasing Laplacian pyramid filters.

5. CONCLUSION

The paper discusses the PDFB for the contourlet transform as an overcomplete FB and shows that the equivalent directional filters of the PDFB suffer from the aliasing effects due to its multiresolution structure. By imposing the conditions that the two lowpass filters of the Laplacian pyramid should have frequency supports restricted within $[-\pi/2, \pi/2]^2$, the aliasing in the stopbands is reduced, except for those in the finest resolution. The findings in this paper can help improve the performance of the PDFB in image processing applications, such as low-bitrate coding and image denoising.

6. ACKNOWLEDGMENT

We would like to thank Dr. Yilong Liu (Video Insight), for providing Fig. 9.

REFERENCES

[1] E. J. Candès and D. L. Donoho, "Curvelets - a surprisingly effective nonadaptive representation for objects with edges," in *Curves and Surfaces*, L. L. S. et al., Ed. Nashville, TN: Vanderbilt University Press, 1999.

[2] S. Mallat, *A Wavelet tour of signal processing*, 2nd ed. Academic Press, 1999.

[3] M. Vetterli, "Wavelets, approximation and compression," *IEEE Signal Processing Magazine*, vol. 18, no. 5, pp. 59–73, 2001.

[4] M. N. Do and M. Vetterli, "The contourlet transform: An efficient directional multiresolution image representation," *IEEE Transactions on Image Processing*, vol. 14, pp. 2107– 2116, Dec. 2005.

[5] P. J. Burt and E. H. Adelson, "The laplacian pyramid as a compact image code," *IEEE Transaction on Communication*, vol. 31, no. 4, pp. 532–540, Apr. 1983.

[6] R. H. Bamberger and M. J. T. Smith, "A filter bank for the directional decomposition of images: theory and design," *IEEE Transactions on Signal Processing*, vol. 40, no. 7, pp. 882 –893, Apr. 1992.

[7] V. Chappelier, C. Guillemot, and S. Marinkovic, "Image coding with iterated contourlet and wavelet transforms," in *Proc. IEEE International Conference on Image Processing, ICIP04*, Singapore, Oct. 2004.

[8] H. Song, S. Yu, L. Song, and H. Xiong, "Contourlet image coding based on adjusted spiht," in *Proc. 6th Pacific Rim Conference on Multimedia, PCM 2005*, ser. Lecture Notes in Computer Science. Springer, Nov. 2005, pp. 629–640.

[9] R. Eslami and H. Radha, "On low bit-rate coding using the contourlet transform," in *Conference Record of the Thirty-Seventh Asilomar Conference on Signals, Systems and Computers, 2003.*, vol. 2, Nov. 2003, pp. 1524– 1528.

[10] P. Vaidyanathan, *Multirate Systems and Filter Banks*. Prentice-Hall,Englewood Cliffs, NJ, 1993.

[11] S. I. Park, M. J. Smith, and R. M. Mersereau, "Improved structure of maximally decimated directional filter banks for spatial image analysis," *IEEE Transactions on Image Processing*, vol. 13, no. 11, pp. 1424 – 1431, Nov. 2004.

[12] S.-M. Phoong, C. Kim, P. Vaidyanathan, and R. Ansari, "A new class of two-channel biorthogonal filter banks and wavelet bases," *IEEE Transactions on Signal Processing*, vol. 43, no. 3, pp. 649–665, Mar. 1995.

[13] Y. Liu, T. T. Nguyen, and S. Oraintara, "Low bitrate image coding based on pyramidal directional filter banks," in *Proc. IEEE International Conference on Acoustics, Speech, and Signal Processing (ICASSP'06)*, France, May 2006.